

very well the idealized disorder case that is often used (Fig. 1). In fact, the structure fabricated by Jang et al. is very thin and consists of a subwavelength array of nanopillars with random widths, which results in very high transverse wavevectors together with a wide memory effect range (that is, adding a phase gradient to the input adds the same phase gradient to the output), a combination that is difficult to achieve with natural or self-assembled systems. While the engineered disordered metasurface doesn't do anything that a conventional thin scattering medium can't do, its strength lies in its simplicity of use and reliability. As the scattering matrix is known a priori, such a metasurface can be used as a wide-field and high-magnification optical component without any characterization (once it is properly aligned). Furthermore, contrary to

many self-assembled systems that tend to drift with time, the engineered metasurface is extremely durable and stable, making it realistic for use as an everyday component, such as in a microscope.

It is still unclear whether it will ever be possible to reliably design and fabricate the full 3D multiply scattering media necessary to control quantum states or the time evolution of laser pulses, but 2D disordered metasurfaces offer many optical functionalities and the freedom to tune them at will. It would be no surprise if such devices became commonplace in tomorrow's microscopes. □

Jacopo Bertolotti

Department of Physics and Astronomy, University of Exeter, Exeter, UK.
e-mail: j.bertolotti@exeter.ac.uk

Published online: 26 January 2018

<https://doi.org/10.1038/s41566-018-0090-y>

References

1. Mosk, A. P., Lagendijk, A., Leroose, G. & Fink, M. *Nat. Photon.* **6**, 283–292 (2012).
2. van Putten, E. G. et al. *Phys. Rev. Lett.* **106**, 193905 (2011).
3. Dholakia, K. & Čížmár, T. *Nat. Photon.* **5**, 335–342 (2011).
4. Freund, I., Rosenbluh, M. & Feng, S. *Phys. Rev. Lett.* **61**, 2328–2331 (1988).
5. Aulbach, J., Gjonaj, B., Johnson, P. M., Mosk, A. P. & Lagendijk, A. *Phys. Rev. Lett.* **106**, 103901 (2011).
6. Carpenter, J., Eggleton, B. J. & Schröder, J. *Nat. Photon.* **9**, 751–757 (2015).
7. Huisman, T. J., Huisman, S. R., Mosk, A. P. & Pinkse, P. W. H. *Appl. Phys. B* **116**, 603–607 (2013).
8. Defienne, H. et al. *Opt. Lett.* **39**, 6090–6093 (2014).
9. Popoff, S. et al. *Phys. Rev. Lett.* **104**, 100601 (2010).
10. Jang, M. et al. *Nat. Photon.* <https://doi.org/10.1038/s41566-017-0078-z> (2018).
11. Beenakker, C. W. J. *Rev. Mod. Phys.* **69**, 731–808 (1997).
12. Freund, I. *Phys. A* **168**, 49–65 (1990).
13. Ben-Avraham, D. & Havlin, S. *Diffusion and Reactions in Fractals and Disordered Systems* (Cambridge Univ. Press, Cambridge, 2000).

OPTICAL PHYSICS

Broadband optomechanical non-reciprocity

Implementing non-reciprocal elements with a bandwidth comparable to optical frequencies is a challenge in integrated photonics. Now, a phonon pump has been used to achieve optical non-reciprocity over a large bandwidth.

Alireza Seif and Mohammad Hafezi

Non-reciprocal elements play an important role in photonic circuits. Two hallmark examples are optical isolators and circulators, where the input–output relations are not symmetric. Specifically, an isolator allows for transport in one direction and suppresses it in the other, and a circulator is essentially a multiport generalization of an isolator. Developing such devices at the microscale is crucial for routing photons and reducing backscattering and parasitic interference effects in integrated photonic circuits.

Non-reciprocity can be achieved by locally breaking time-reversal symmetry. For example, time-reversal symmetry can be broken by applying a magnetic field in materials with strong magneto-optical responses. A Faraday rotator is an example of such a device that rotates the polarization of light in a non-reciprocal fashion. However, due to the weakness of the magneto-optical effect in materials used in nanophotonics as well as the difficulties in controlling large magnetic fields at small length scales, this approach may not be suitable for engineering on-chip non-reciprocity.

In recent years, there has been an active search for alternatives to magneto-optical non-reciprocity. In a seminal work published in 2009, Yu and Fan proposed that isolation in a nanophotonic system can be achieved by modulating the refractive index of the material¹. The modulation provides the momentum and energy required for an interband photonic transition. Specifically, because of the phase-matching condition, the transition is only allowed for photons travelling in one direction and is non-reciprocal. This proposal was implemented in 2012 in an electrically driven silicon chip². In the same year, it was proposed that non-reciprocity can also be achieved in optomechanical systems³. In this scheme, non-reciprocal interactions are realized by selective enhancement of the optomechanical coupling in one direction by optical pumping.

Recently, this proposal was implemented in a whispering gallery microresonator⁴ and later generalized to other optomechanical systems⁵. Previous optomechanical implementations have relied on optical modulation with a laser to achieve non-

reciprocity^{4–6}. In these approaches, the bandwidth of the non-reciprocal behaviour is limited to the kHz–MHz range by the width of the mechanical oscillator resonance.

As reported in *Nature Photonics*, Donggyu Sohn and colleagues from the University of Illinois at Urbana-Champaign have now successfully used mechanical modulations to achieve non-reciprocity over a large GHz bandwidth⁷. Reversing the role of mechanical and optical modes allows the bandwidth to be dictated by the optical loss, which is orders of magnitude larger than its mechanical counterpart.

Sohn et al. used an optomechanical resonator that supports two optical modes (Fig. 1a). Because of the photoelastic effect, these optical modes couple to acoustic waves that are pumped into the structure. The strength of this three-way interaction depends on the overlap of the optical modes and the mechanical displacements. Therefore, when the acoustic mode is modulated, this interaction can lead to a simultaneous absorption of an optical excitation in one of the modes and a mechanical excitation and an optical

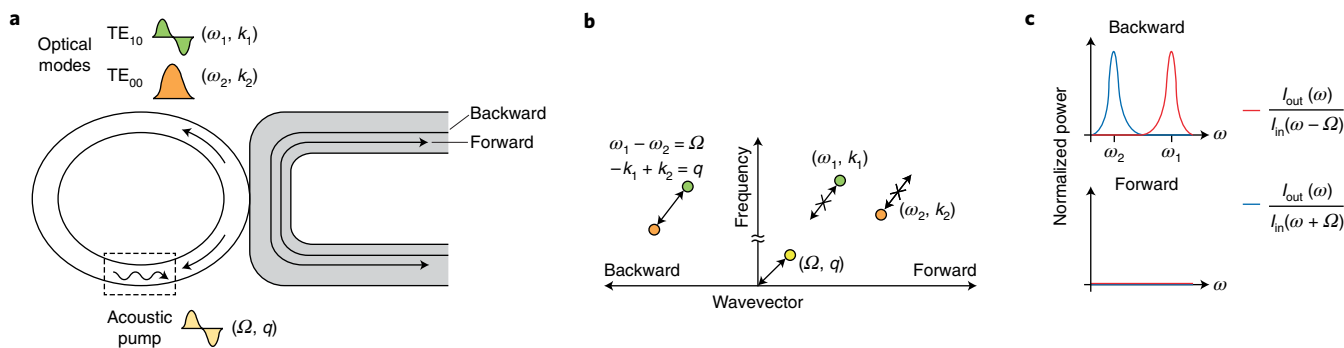


Fig. 1 | The experimental set-up and non-reciprocal interband transition scheme. **a**, The set-up consists of a racetrack resonator coupled to a waveguide supporting the lower momentum TE_{10} (green) mode with frequency and momentum ω_1, k_1 and the higher momentum TE_{00} (orange) mode with ω_2, k_2 . By acoustically pumping (yellow) the resonator with frequency and momentum, Ω, q , in one direction, the optical field experiences a frequency shift only in the preferred direction. **b**, When $\omega_1 > \omega_2$, the phase-matching condition is only satisfied in the backward direction for acoustic pumping in the forward direction, that is, $\omega_1 - \omega_2 = \Omega$ and $-k_1 + k_2 = q$. **c**, The normalized power of down-converted Stokes (blue) and up-converted anti-Stokes (red) sidebands. Because of the phase-matching condition, the TE_{10} and TE_{00} modes convert to each other in the backward direction, while this conversion does not occur in the forward direction. Figure adapted from ref. ⁷, Macmillan Publishers Ltd.

emission into the other, hence causing an indirect interband scattering. The phase and momentum of the pump can be tailored such that the phase-matching condition is only satisfied in one direction. Therefore, the device acts as a non-reciprocal modulator, that is, only the light propagating in the designated direction is converted to a different mode and experiences a frequency shift (Fig. 1b).

The racetrack resonator used by Sohn et al. is fabricated from aluminium nitride (AlN) on a silicon substrate. This choice of material offers suitable optical and acoustic properties, and allows for piezoelectric driving of the acoustic mode. The resonator, which is a wrapped ridge waveguide, supports quasi- TE_{10} and quasi- TE_{00} optical modes around 1,550 nm, while all the other modes are suppressed by limiting the dimensions of the resonator. To pump the acoustic mode, the researchers utilized an interdigitated transducer (IDT) fabricated on the same AlN substrate. By adding a free edge reflector to the angled IDT set-up, they could satisfy momentum constraints in both transverse and propagating directions. The former guarantees a non-zero optomechanical coupling, while the latter ensures the phase-matching condition is satisfied. The frequency of the acoustic drive is fixed at $\Omega = 4.82$ GHz in the experiment, and approximately satisfies the frequency-matching condition for the first pair of modes that the researchers considered.

To probe the system, a linear waveguide is evanescently coupled to the resonator at a single point. The input optical field

with power $I_{in}(\omega)$ is swept at frequency ω , and the transmitted power of the down-converted Stokes ($I_{out}(\omega - \Omega)$) and the up-converted anti-Stokes ($I_{out}(\omega + \Omega)$) sidebands are measured simultaneously (Fig. 1c). In the case of perfect phase-matching for a backward-propagating probe signal, Sohn and colleagues observed the expected intermodal scattering with a -3 dB bandwidth of 1.14 GHz. The sidebands generated for the opposite direction are 15 dB smaller. While these sidebands should ideally be zero, there are inevitable experimental limitations such as misalignment and curvature of the racetrack resonator that lead to intramodal scatterings. The researchers also showed that for other mode pairs, when the frequency matching is not satisfied, the non-reciprocal sideband generation, though less prominent, still exists.

To assess the maximum mode conversion efficiency, that is, the ratio of the power of a sideband to the input power, the researchers fixed the probe laser in the backward direction for the phase-matched modes, with a frequency where the anti-Stokes sideband generation is maximized. They varied the acoustic pump's power and showed that the conversion efficiency follows the expected behaviour and increases with the pump's power. However, there is a limit to this efficiency, and pumping beyond this limit would split the modes and put the system in the strong-coupling regime. This regime could not be reached due to experimental limitations of the IDT power. However, the fact that the system follows the expected behaviour with the drive power suggests

that the strong-coupling regime should be obtainable in the future.

The modulator that Sohn et al. demonstrated is an interesting magnetic-free non-reciprocal device that uses phonons instead of photons to stimulate the optomechanical interaction. With a rise time of a few nanoseconds, it could serve as an on-chip frequency shifter. As the next step, it would be interesting to achieve the strong-coupling regime in the set-up and extend these techniques to demonstrate linear isolators and circulators that operate over a large bandwidth with low insertion loss. A large-bandwidth non-reciprocal device with small footprint that is CMOS compatible would open up new opportunities in integrated photonics. In addition, since this scheme is an effective linear optical conversion, it could, in principle, work at the quantum limit, and could be used for quantum-information-processing tasks. \square

Alireza Seif and Mohammad Hafezi*

University of Maryland, College Park, MD, USA.

*e-mail: hafezi@umd.edu

Published online: 26 January 2018

<https://doi.org/10.1038/s41566-018-0091-x>

References

1. Yu, Z. & Fan, S. *Nat. Photon.* **3**, 91–94 (2009).
2. Lira, H. et al. *Phys. Rev. Lett.* **109**, 033901 (2012).
3. Hafezi, M. & Rabl, P. *Opt. Express* **20**, 7672–7684 (2012).
4. Shen, Z. et al. *Nat. Photon.* **10**, 657–661 (2016).
5. Fang, K. et al. *Nat. Phys.* **13**, 465–471 (2017).
6. Kim, J. et al. *Nat. Phys.* **11**, 275–280 (2015).
7. Sohn, D. B., Kim, S. & Bahl, G. *Nat. Photon.* <https://doi.org/10.1038/s41566-017-0075-2> (2018).